

A Study on Temperature Distributions in a Stratified Thermal Storage Tank

Monton Jaikuson

Department of Mechanical Engineering, Faculty of Engineering, King Mongkut Institute of Technology Ladkrabang
Chalongkrung Rd. Ladkrabang Bangkok 10520 Thailand
Tel 0-2326-4197 Fax: 0-2326-4198 E-mail : kjmonton@kmitl.ac.th

Abstract

This paper describes the effect of three different diffusers on a temperature distribution of water in a stratified storage tank. The different diffusers used in the experiment are (1) diffuser with a single jet, (2) lightly perforated diffuser, (3) highly perforated diffuser. A two dimensional, unsteady mathematical model has been developed with Finite Volume technique based on QUICK scheme. The temperature distributions are obtained numerically that are in agreement with experimental data. The results show that the highly perforated diffuser can store more energy in the storage tank than the lightly perforated diffuser, and a diffuser with a single jet is not suitable to store the energy in comparison with the two perforated diffusers.

1. Introduction

Thermal stratification in enclosure can be found in many engineering applications. For example, a stratified chilled water tank can be utilized in air conditioning equipment. Another example is the storage of hot water from solar collectors. The simplest storage design is a single liquid contained in a tank within which stratification is maintained by utilizing the density difference between hot and cold liquid layers. Thus the single stratified tank is the most attractive choice due to its simplicity and low cost. The stratified hot water can make solar energy available at night in housing and factory for heating. The stratification in a storage tank could be influenced by (1) thermal mixing at inlet and outlet, (2) tank geometry, (3) heat diffusion due to temperature gradient, (4) force convection flow through storage tank, and (5) heat loss to ambient air. From the key factors as mentioned above, the design of a storage tank to ensure high efficiency is important. In this paper, some inlet configurations in a storage tank are experimentally considered.

There have been many studies on stratified storage tanks. Hariharan et al [1] realized experiments on stratified storage tanks to study the effects of operating conditions on the thermoclines and on the extraction efficiency. Ghajar and Zurigat [2] realized a numerical study of the effect of inlet geometry on

stratification in thermal energy storage. Abu-Hamdan et al [3] presented an extensive experimental study to evaluate the thermal performance of a stratified storage tank under variable inlet temperature conditions. Al-Najem [4] investigated the thermal stratification in storage tank using a theoretical model based on an integral transform technique. Kleinbach et al [5] developed two basic approaches to study the thermal stratification in thermal storage tanks, and the results of storage tank models were compared with experimental data.

This attention is focused on the effect of different perforated diffusers, and diffuser with a symmetrical jet on the temperature distributions. The numerical solutions using Finite Volume Method based on QUICK scheme with a two-dimensional two-equation turbulence model ($k - \epsilon$ model) are also made in order to compare with the experimental data when inlet diffuser is a symmetrical jet.

2. Mathematical Models

2.1 Common Form of Governing Equations

All the governing partial differential equations shown in appendix can be reorganized and expressed in a standard form that includes the convection, diffusion, and source terms for 2-D axisymmetric flow as follows[6];

$$\frac{\partial(\bar{\rho}\phi)}{\partial t} + \frac{\partial(\bar{\rho}\tilde{u}\phi)}{\partial x} + \frac{\partial(r\bar{\rho}\tilde{v}\phi)}{r\partial r} = \frac{\partial}{\partial x} \left[\Gamma_{\phi x} \frac{\partial\phi}{\partial x} \right] + \frac{\partial}{r\partial r} \left[r\Gamma_{\phi r} \frac{\partial\phi}{\partial r} \right] + S_{\phi} \quad (1)$$

Where ϕ stands for any variable, Γ_{ϕ} are the exchange coefficients for ϕ , and S_{ϕ} is source term, which are classified;

2.1.1 Continuity Equation

$$\begin{aligned} \phi &= 1 \\ \Gamma_{\phi x} &= 0 \\ \Gamma_{\phi r} &= 0 \\ S_{\phi} &= 1 \end{aligned} \quad (2)$$

2.1.2 Momentum Equation

$$\begin{aligned} \phi &= \tilde{u} \\ \Gamma_{\phi x} &= \mu + \mu_t \\ \Gamma_{\phi r} &= \mu + \mu_t \end{aligned} \quad (3)$$

$$S_{\phi} = \frac{\partial}{\partial x} \left[(\mu + \mu_t) \frac{\partial\tilde{u}}{\partial x} \right] + \frac{\partial}{r\partial r} \left[(\mu + \mu_t) r \frac{\partial\tilde{v}}{\partial r} \right] - \frac{\partial\bar{p}}{\partial x} - \frac{2\bar{\rho}\partial k}{3\partial x} - (\bar{\rho} - \bar{\rho}_0)g$$

and

$$\begin{aligned} \phi &= \tilde{v} \\ \Gamma_{\phi x} &= \mu + \mu_t \\ \Gamma_{\phi r} &= \mu + \mu_t \end{aligned} \quad (4)$$

$$S_{\phi} = \frac{\partial}{\partial x} \left[(\mu + \mu_t) \frac{\partial\tilde{u}}{\partial r} \right] + \frac{\partial}{r\partial r} \left[(\mu + \mu_t) r \frac{\partial\tilde{v}}{\partial r} \right] - \frac{\partial\bar{p}}{\partial r} - \frac{2\bar{\rho}\partial k}{3\partial r} - \frac{2(\mu + \mu_t)\tilde{v}}{r^2}$$

2.1.3 Energy Equation

$$\begin{aligned} \phi &= \bar{H} \\ \Gamma_{\phi x} &= \left(\frac{\mu}{\sigma_{T,l}} + \frac{\mu_t}{\sigma_{T,t}} \right) \\ \Gamma_{\phi r} &= \left(\frac{\mu}{\sigma_{T,l}} + \frac{\mu_t}{\sigma_{T,t}} \right) \\ S_{\phi} &= 0 \end{aligned} \quad (5)$$

2.1.4 Turbulent Kinetic Energy Equation

$$\begin{aligned} \phi &= k \\ \Gamma_{\phi x} &= \left(\frac{\mu_t}{\sigma_k} + \mu \right) \\ \Gamma_{\phi r} &= \left(\frac{\mu_t}{\sigma_k} + \mu \right) \end{aligned}$$

$$S_{\phi} = \mu \left[2 \left(\left(\frac{\partial\tilde{u}}{\partial x} \right)^2 + \left(\frac{\partial\tilde{v}}{\partial r} \right)^2 + \left(\frac{\tilde{v}}{r} \right)^2 \right) + \left(\frac{\partial\tilde{u}}{\partial r} + \frac{\partial\tilde{v}}{\partial x} \right)^2 \right] + \beta g \frac{\mu}{\sigma_{T,t}} \frac{\partial\bar{T}}{\partial x} - \bar{\rho}\epsilon \quad (6)$$

2.1.5 Dissipation Equation

$$\begin{aligned} \phi &= \epsilon \\ \Gamma_{\phi x} &= \left(\frac{\mu_t}{\sigma_{\epsilon}} + \mu \right) \\ \Gamma_{\phi r} &= \left(\frac{\mu_t}{\sigma_{\epsilon}} + \mu \right) \end{aligned} \quad (7)$$

$$S_{\phi} = C_{\epsilon 1} \frac{\epsilon}{k} (G+B) (1+C_3 R_f) - C_{\epsilon 2} \bar{\rho} \frac{\epsilon^2}{k}$$

2.2 Discretization of the equations

The discretized unsteady form of the partial differential equations, [equation2-7], can be obtained by combining the discretized unsteady, convection, diffusion, and source terms together with QUICK and implicit schemes as follows;

$$a_p \phi_p = a_w \phi_w + a_E \phi_E + a_S \phi_S + a_N \phi_N + a_p^{\circ} \phi_p^{\circ} + \bar{S}_U \quad (8)$$

Where $a_p = a_w + a_E + a_S + a_N + a_p^{\circ} - S_p$

$$\text{And } a_p^{\circ} = \frac{\rho^{\circ} \phi_p^{\circ}}{\Delta t}$$

2.2.1 QUICK scheme

This QUICK scheme [6] uses a quadratic interpolation between two upstream neighbors and one downstream neighbor in order to approximate the ϕ value at a control volume interface. Depending on the sign of the flux at the interface as shown in Figure 1. For instance the quadratic interpolation for a grid at the east face becomes

$$\phi_e = \begin{cases} \phi_p + \frac{1}{8}(3\phi_E - 2\phi_p - \phi_W), C_e > 0 \\ \phi_E + \frac{1}{8}(3\phi_p - 2\phi_E - \phi_{EE}), C_e < 0 \end{cases} \quad (9)$$

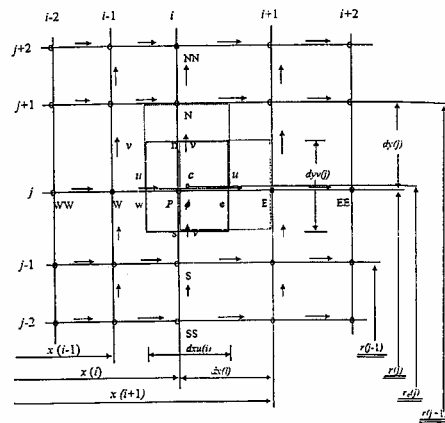


Figure 1 Circular grid arrangement and layout of variables

3. Experiments

The experimental measurements of temperature distribution of water in an insulated cylindrical storage tank were made with three different diffusers as shown in Figure 2. Three different diffusers in the insulated storage tank are selected for experimentation and all diffusers are insulated and installed within a top of the tank. The first diffuser has an inlet big hole of 39 mm diameter in a center point. The second diffuser is called "Lightly Perforated Diffuser" 500 mm in diameter with a very small hole diameter of 2 mm, and 537 holes in the diffuser. Finally the third diffuser called "Highly Perforated Diffuser" has 500 mm diameter and 921 holes in the diffuser with the same hole diameter as that of the second diffuser. The three different diffusers are shown in Figure 2b and 2c.

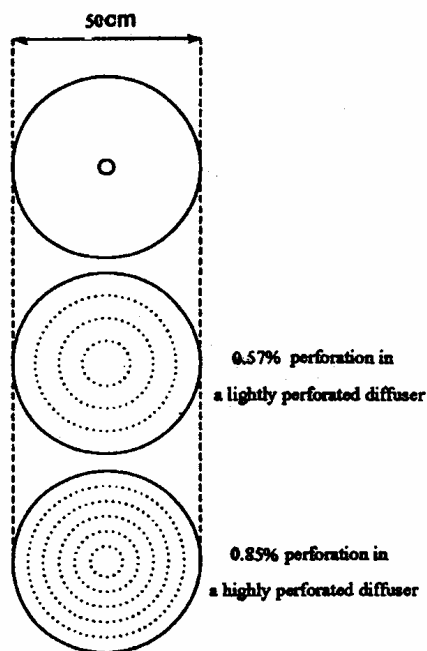


Figure 2 Three different diffusers, (a) Diffuser with a single jet (b) Lightly Perforated Diffuser (c) Highly Perforated Diffuser

The experimental storage tank has in 500 mm in diameter, and 1600 mm in height. Eight and seven locations of K – Type thermocouple probes are placed in a centerline and a radius 15 cm respectively. They are shown in Figure 3.

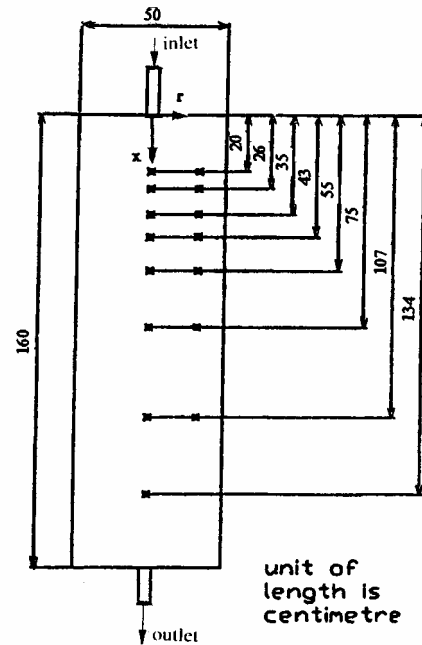


Figure 3 The locations of thermocouples

4. Results and Discussion

The experimental results of temperature distributions of water in the storage tank are only shown for a centerline location. The input temperature of hot water and an initial temperature of cold water are used in this experiment as 335 K and 304 K respectively.

4.1 Relation of temperature distributions between a diffuser with single jet and a lightly perforated diffuser

Temperature distributions in a diffuser with a single jet and a lightly perforated diffuser are evidently different as shown in Figure 4. It shows that the storage tank charged with the diffuser with a single jet can increase more a mixing effect on a vertical layer than the lightly perforated diffuser. So the effect of two heat transfer mechanisms the diffuser with a single jet, namely, thermal convection and thermal diffusion, rapidly expands to a vertically thermal layer in short time when using diffuser with a single jet. While the type of perforated diffuser can obviously inhibit the effect of thermal convection through a bottom region of storage tank. It makes a mixing zone happening in a top region, and finally an accumulated energy in the top region is increased according to a passing time. As the results, a using of the diffuser with a single jet makes a stratification in storage tank worst in comparison with the perforated diffuser.

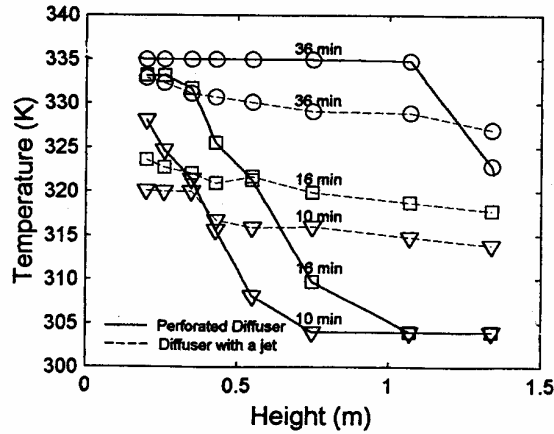


Figure 4 Comparison of temperature distributions in diffuser with a single jet and in perforated diffuser when a flow rate 8.28 L/min

4.2 Relation of temperature distribution between a lightly and a highly perforated diffuser for low flow rate

In Figure 5, at low flow rate, the tendencies of temperature distributions in using a lightly perforated diffuser are the same as those in a highly perforated diffuser. It is evident that a type of two experimentally perforated diffusers does not effect on temperature distributions in storage tank when the flow rate is very low. The reason is that the behaviors of mixing between hot water and cold water in the storage tank are similar when using two perforated diffusers. So the effect of buoyancy force has more dominantly affected than the type of the two perforated diffusers.

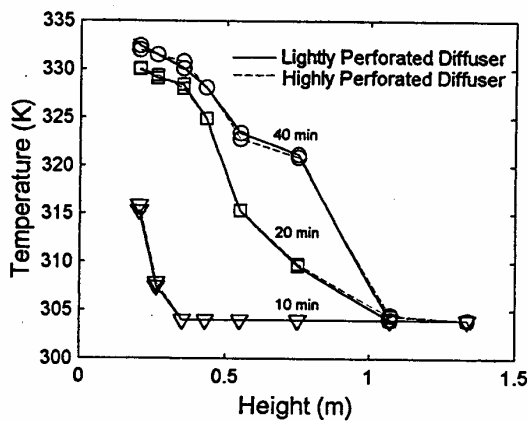


Figure 5 Comparison of temperature distributions in a lightly perforated diffuser and a highly perforated diffuser when a flow rate 4.59 L/min

4.3 Relation of temperature distribution between a lightly and a highly perforated diffuser for medium flow rate

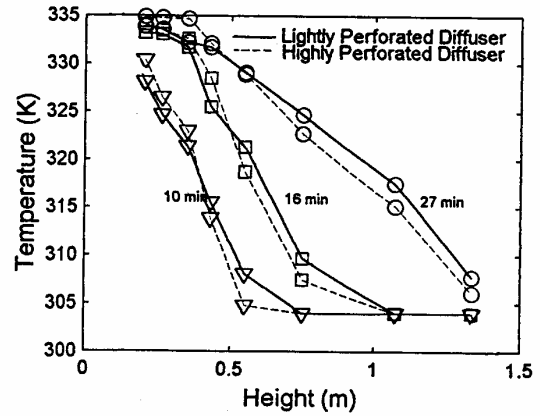


Figure 6 Comparison of temperature distributions in a lightly perforated diffuser and a highly perforated diffuser when a flow rate 8.28 L/min

As shown in Figure 6, the tendencies of temperature distribution in lightly perforated diffuser are similar to those in highly perforated diffuser. In the same time, a highly perforated diffuser can produce better a stratification in storage tank than a lightly perforated diffuser. It shows that the medium flow rate has more effect on the temperature distribution than the low flow rate. And this flow rate also define a type of two perforated diffusers which effects on the stratification. The reason of the results is that a highly perforated diffuser can reduce the mixing in a top region of storage tank in comparison with a lightly perforated diffuser. As the result, a number of holes in highly perforated diffuser can distribute more the flow rate through the cross sectional area of storage tank than that in lightly perforated diffuser.

4.4 Relation of temperature distribution between a lightly and a highly perforated diffuser for high flow rate

Figure 7 gives a plot of temperature distributions and a height of storage tank when a flow rate is high. It is found that the tendencies of temperature distribution in this case are slightly different from those of Figure 6. A highly perforated diffuser, in the same time, almost products better a stratification in storage tank than a lightly perforated diffuser. Some interesting results are found that the high flow rate does not make a stratification better than the medium flow rate dominantly. For example, especially at time 7 and 10 min, the highly perforated diffuser does not make the better stratified than the lightly perforated diffuser, which is unlike Figure 6. It shows that each thermal layer of water in storage tank is in disorder because flow rates through holes in the perforated diffuser is very high. So the flow rates can increase the mixing between hot and cold water in storage tank. Finally they do not make the stratification better

although an input energy to storage tank due to a high flow rate is increased.

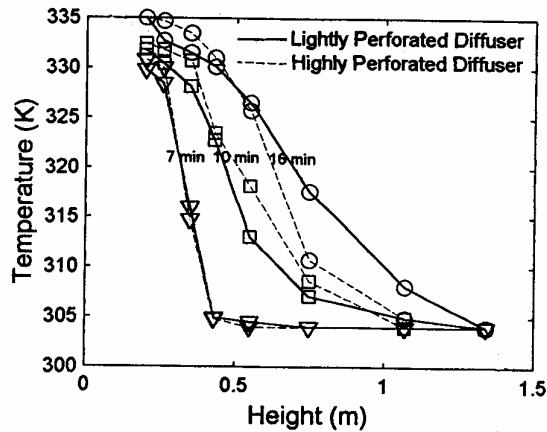


Figure 7 Comparison of temperature distributions in a lightly perforated diffuser and a highly perforated diffuser when a flow rate 14.53 L/min

4.5 Results of numerical and experimental solution

The calculated temperature distributions in flow rate 14.53 L/min and inlet temperature 335 K with QUICK scheme are shown in Figure 8. Figure 8(a) and Figure 8(b) represent the comparison of calculation and experiment in diffuser with a single jet at a location of centerline and a location of radius 15 cm respectively when the time is 10 min. Numerical solutions in Figure 8 are based on a 52x27 non-uniform grid. From the Figure 8, It is found that the graph for calculation of temperature distribution in centerline is close to the experimental results. Although temperature distributions in the location of radius 15 cm are slightly different, the tendency of temperature distributions is in agreement to the experimental data. The turbulent flow in the storage tank can be found from the graph of regimes of flow in vertical tubes [Adapted from B. Metais and E.R.G. Eckert, Trans. ASME, Ser. C, Journal of Heat Transfer, 86 : 295 (1964).].

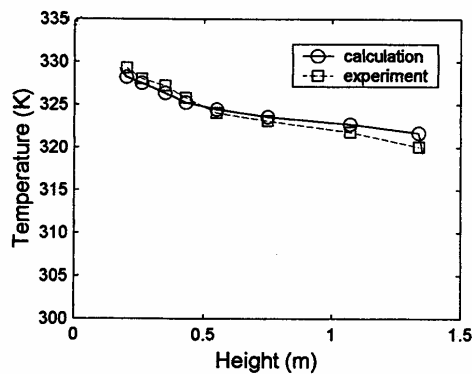


Figure 8 (a) Comparison of calculation and experiment in diffuser with a single jet at centerline when the time is 10 min

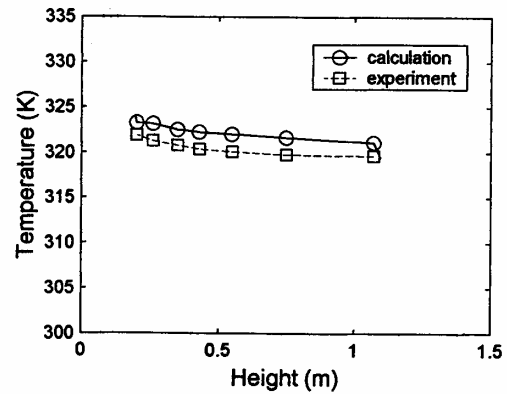


Figure 8 (b) Comparison of calculation and experiment in diffuser with a single jet at radius 15 cm when the time is 10 min

5. Conclusion

This paper is carried out in order to provide an understanding of the significant effect on a temperature in a stratified storage tank when different diffusers are reshuffled. It is shown in two perforated diffusers that for low flow rate, temperature distributions in a lightly perforated diffuser are the same as those in a highly perforated diffuser. When a flow rate is increased (8.28 L/min), a stratification in the highly perforated diffuser is better than that in the lightly perforated diffuser. Finally if the flow rate is increased (14.53 L/min), it is still to make the same stratified as the medium flow rate. In case of using the diffuser with a single jet, It is found that a stratification in storage tank behaves worse in comparison with using the two perforated diffusers. For the numerical solutions from Finite Volume Method with QUICK scheme, they are in agreement to the calculation solutions.

6. Symbols

a	coefficient in discretization equation
B	generation term relating buoyancy
c_p	specific heat coefficient
$C_{\epsilon 1}, C_{\epsilon 2}$	constants in dissipation rate equation
c_μ	constant in the $k - \epsilon$ equation
c	convection term
G	generation term
\tilde{H}	mean total enthalpy
k	turbulence kinetic energy
k_T	thermal conductivity
\bar{p}	mean pressure
r	radial coordinate
S_ϕ	source term
S_U, S_p	constant part of and coefficient in the

	linearised source term respectively
t	time
\bar{T}	mean temperature
\tilde{u}	mean velocity in x-direction
\tilde{v}	mean velocity in r-direction
x	axial coordinate

6.1 Greek Symbols

β	volumetric expansion coefficient
ε	dissipation
ϕ	scalar property
Γ_ϕ	exchange coefficient with property ϕ
μ, μ_t	laminar viscosity, turbulent viscosity
$\rho, \bar{\rho}$	density, mean density
$\sigma_{T,l}$	laminar Prandtl number
$\sigma_{T,t}$	turbulent Prandtl number

6.2 Subscripts

P	node P
N	neighboring point on north side
W	neighboring point on west side
E	neighboring point on east side
S	neighboring point on south side
t	turbulence

6.3 Superscripts and overbars

-	time averaged mean value
o	initial field

7. References

- [1] Hariharan, K., Badrinarayana, K., Murthy, S. S. and Murthy, M. V.K., Energy-The International Journal, Vol 16 (1991), pp.977
- [2] Y.H. Zurigat, A.J Ghajar, Stratified Thermal Storage Tank Inlet Mixing Characterization, Applied Energy, Vol 30(1988), pp. 99-111.
- [3] Abu-Hamdan, M.G.,Zurigat, Y.H., Numerical Heat Transfer, Part A, 1991, Vol 19, pp. 65.
- [4] N.M. Al-Najem and M.M. El-Refaee, A Numerical Study for the Prediction of Turbulent Mixing Factor in Thermal Storage Tanks, Applied Thermal Engineering, Vol 17 (1997), pp. 1173-1181.
- [5] Kleinbach, E.M., Beckman, W.A. and Klein, S. A.,Two Basic Approaches to study the thermal stratification in Thermal Storage Tanks, Solar Energy, Vol 50 (1993), pp155
- [6] Versteeg H.K. and Malalasekera W., An Introduction to Computational Fluid Dynamics, The Finite Volume Method,

Longman Scientific & Technical, Longman Group (1995), English.

8. Appendix

The governing equations for this transient process involving the stratified storage tank consist of the equations for time-averaged continuity, momentum, energy, turbulent energy k , and dissipation rate of the turbulent energy ε . A two-dimensional cylindrical coordinate system can be expressed as follows;

$$\frac{\partial(r\bar{\rho}\tilde{v})}{r\partial r} + \frac{\partial\bar{\rho}\tilde{u}}{\partial x} + \frac{\partial\bar{\rho}}{\partial t} = 0 \quad (1)$$

$$\frac{\partial(r\bar{\rho}\tilde{u})}{\partial t} + \frac{\partial\bar{\rho}\tilde{u}\tilde{v}}{\partial x} + \frac{\partial(r\bar{\rho}\tilde{u}\tilde{v})}{r\partial r} = \frac{2\bar{\rho}\partial k}{3\partial x} - (\bar{\rho} - \bar{\rho}_0)g - \frac{\partial\bar{p}}{\partial x} + \frac{\partial}{\partial x} \left[2(\mu + \mu_t) \frac{\partial\tilde{u}}{\partial x} \right] + \frac{\partial}{\partial r} \left[(\mu + \mu_t) r \left(\frac{\partial\tilde{u}}{\partial r} + \frac{\partial\tilde{v}}{\partial x} \right) \right] \quad (2)$$

$$\frac{\partial(\bar{\rho}\tilde{v})}{\partial t} + \frac{\partial\bar{\rho}\tilde{u}\tilde{v}}{\partial x} + \frac{\partial(r\bar{\rho}\tilde{v}\tilde{v})}{r\partial r} = \frac{2\bar{\rho}\partial k}{3\partial r} - \frac{2(\mu + \mu_t)v}{r^2} - \frac{\partial\bar{p}}{\partial r} + \frac{\partial}{\partial x} \left[(\mu + \mu_t) \frac{\partial\tilde{u}}{\partial r} + \frac{\partial\tilde{v}}{\partial x} \right] + \frac{\partial}{\partial r} \left[2(\mu + \mu_t) r \frac{\partial\tilde{v}}{\partial r} \right] \quad (3)$$

$$\frac{\partial\bar{\rho}(c_p\bar{T})}{\partial t} + \frac{\partial\bar{\rho}(\tilde{u}c_p\bar{T})}{\partial x} + \frac{\partial\bar{\rho}(r\tilde{v}c_p\bar{T})}{r\partial r} = \frac{\partial}{\partial x} \left[\left(k_r + \frac{c_p\mu_t}{\sigma_{T,t}} \right) \frac{\partial\bar{T}}{\partial x} \right] + \frac{\partial}{\partial r} \left[\left(k_r + \frac{c_p\mu_t}{\sigma_{T,t}} \right) r \frac{\partial\bar{T}}{\partial r} \right] \quad (4)$$

$$\frac{\partial(\bar{\rho}k)}{\partial t} + \frac{\partial(\bar{\rho}\tilde{u}k)}{\partial x} + \frac{\partial(r\bar{\rho}\tilde{v}k)}{r\partial r} = \beta g \frac{\mu_t}{\sigma_{T,t}} \frac{\partial\bar{T}}{\partial x} - \rho\varepsilon + \frac{\partial}{\partial x} \left[\left(\frac{\mu_t}{\sigma_k} + \mu \right) \frac{\partial k}{\partial x} \right] + \frac{\partial}{\partial r} \left[\left(\frac{\mu_t}{\sigma_k} + \mu \right) r \frac{\partial k}{\partial r} \right] + \mu_t \left[2 \left(\frac{\partial\tilde{u}}{\partial x} \right)^2 + \left(\frac{\partial\tilde{v}}{\partial r} \right)^2 + \left(\frac{\tilde{v}}{r} \right)^2 \right] + \left(\frac{\partial\tilde{u}}{\partial r} + \frac{\partial\tilde{v}}{\partial x} \right)^2 \quad (5)$$

$$\frac{\partial(\bar{\rho}\varepsilon)}{\partial t} + \frac{\partial(r\bar{\rho}\tilde{u}\varepsilon)}{\partial x} + \frac{\partial(r\bar{\rho}\tilde{v}\varepsilon)}{r\partial r} = \frac{\partial}{\partial x} \left[\left(\frac{\mu_t}{\sigma_\varepsilon} + \mu \right) \frac{\partial\varepsilon}{\partial x} \right] + \frac{\partial}{\partial r} \left[\left(\frac{\mu_t}{\sigma_\varepsilon} + \mu \right) r \frac{\partial\varepsilon}{\partial r} \right] + C_{\varepsilon 1} \frac{\varepsilon}{k} (G+B) (1+C_3R_\gamma) - C_{\varepsilon 2} \bar{\rho} \frac{\varepsilon^2}{k} \quad (6)$$

$$\text{where } G = \mu_t \left[2 \left(\left(\frac{\partial\tilde{u}}{\partial x} \right)^2 + \left(\frac{\partial\tilde{v}}{\partial r} \right)^2 + \left(\frac{\tilde{v}}{r} \right)^2 \right) + \left(\left(\frac{\partial\tilde{u}}{\partial r} \right) + \left(\frac{\partial\tilde{v}}{\partial x} \right) \right)^2 \right]$$

$$\text{and } B = \beta g \frac{\mu_t}{\sigma_{T,t}} \left(\frac{\partial\bar{T}}{\partial x} \right)$$

The recommended values of the parameters in $k - \varepsilon$ turbulence model[6] are defined as

$$\sigma_k = 1.0 \quad \sigma_\varepsilon = 1.3 \quad c_{\varepsilon 1} = 1.44$$

$$c_{\varepsilon 2} = 1.92 \quad c_\mu = 0.09 \quad \text{and} \quad \mu_t = \frac{c_\mu \rho k^2}{\varepsilon}$$